AJNR

Preliminary clinical results of proton (1H) imaging of cranial neoplasms: in vivo measurements of T1 and mobile proton density.

T J Brady, F S Buonanno, I L Pykett, P F New, K R Davis, G M Pohost and J P Kistler

Preliminary Clinical Results of Proton (¹H) Imaging of Cranial Neoplasms: In vivo Measurements of T_1 and Mobile Proton Density

Thomas J. Brady,[1] Ferdinando S. Buonanno,[2] Ian L. Pykett,[1] Paul F. J. New,[1] Kenneth R. Davis,[1] Gerald M. Pohost,[3] and J. Philip Kistler[2]

Proton nuclear magnetic resonance (NMR) images reflecting T_1 relaxation time and approximating proton density were acquired and used to generate T_1 rate ($1/T_1$) maps. By region-of-interest selection, measurements of T_1 relaxation time were made from discrete volumes of the imaging plane. Such techniques were applied to the study of human cranial neoplasia and associated conditions of differential diagnostic importance (e.g., postoperative changes, radiation necrosis). Inversion-recovery NMR images exhibit a high lesion-detection sensitivity. In all patients, the specificity of NMR imaging is low since all abnormal areas appear as lesions darker than surrounding normal brain, reflecting a decreased proton density, prolonged T_1 values, or both. T_1 relaxation times are prolonged within neoplastic foci; however, absolute T_1 values overlap with those found in other lesions.

During the last decade, in vitro nuclear magnetic resonance (NMR) spectroscopic studies by several investigators [1–3] have demonstrated prolonged proton T_1 relaxation times in various malignant tissues when compared with values obtained from normal tissue. Prolongation of T_1 in tumors has been associated with, among other things, an increase in tissue water content [4]; however, the mechanism producing this phenomenon has not been fully elucidated.

In this preliminary study, NMR images were obtained that provide both subjective assessment and quantitative measurements of T_1 relaxation time of normal and pathologic brain structures. This approach attempts to determine the utility of NMR imaging in detecting central nervous system (CNS) tumors and related diagnostic problems and to determine whether the detected lesions have specific NMR characteristics.

Materials and Methods

The study population comprised four patients with CNS tumors and three patients with related problems, including radiation necrosis, abscess, and postoperative changes. All patients had routine and neurologic history and physical examination, laboratory studies, and computed tomography (CT). Informed consent, according to the guidelines of the Massachusetts General Hospital Subcommittee of Human Studies, was obtained from all patients before NMR

study. Histopathologic confirmation of the diagnosis was obtained in six patients.

NMR images were obtained using a prototype head imaging system developed by Technicare Corp. (Solon, OH). A static magnetic field of 0.147 tesla, corresponding to a proton resonance frequency of 6.26 MHz, is generated by a four coil, resistive electromagnet. True three-dimensional volumetric data are acquired using two combined radiofrequency (RF) pulse sequences, as previously reported [5]. Postprocessing of the data allows reconstruction of images in any arbitrary plane, including levels corresponding to those of CT scans. Reconstruction of data from a saturation recovery-type technique with the 90°–90° interpulse delay τ set to 1 sec generates images where the signal intensity is mainly dependent on mobile proton density (PD). Reconstruction of data from an inversion-recovery (IR) type of sequence with the 180°–90° interpulse delay τ set to 400 msec provides images that are heavily T_1-weighted. The spatial resolution is about 3–4 mm and is isotropic, that is, equal in all directions.

Results and Discussion

Figure 1 contains representative images through a ventricular plane in a normal volunteer. The image that approximates PD (fig. 1A) has uniform signal intensity within the brain parenchyma but has decreased signal intensity in regions of markedly prolonged T_1, such as cerebrospinal fluid (CSF). The skull appears dark because of decreased mobile proton concentration. In the IR image (fig. 1B), the signal intensity is highly weighted with T_1 information, which provides excellent tissue discrimination. Subcutaneous fat, with its short T_1, appears bright; white matter, gray matter, and CSF, with progressively longer T_1 values, exhibit decreasing intensities.

The T_1 rate image (map) (fig. 1C) closely resembling the IR image, has signal intensity that is inversely proportional to T_1 relaxation times in milliseconds, with short T_1 values appearing bright. The T_1 rate map is computer-generated pixel by pixel from the PD and IR images. Using region-of-interest selection, T_1 relaxation time is measured directly from any desired area on the T_1 map.

The images in figure 2 are from a patient with a clinical history and neurodiagnostic evaluation strongly suggestive of glioma. Unfortunately, this is the only case in this series from whom histopath-
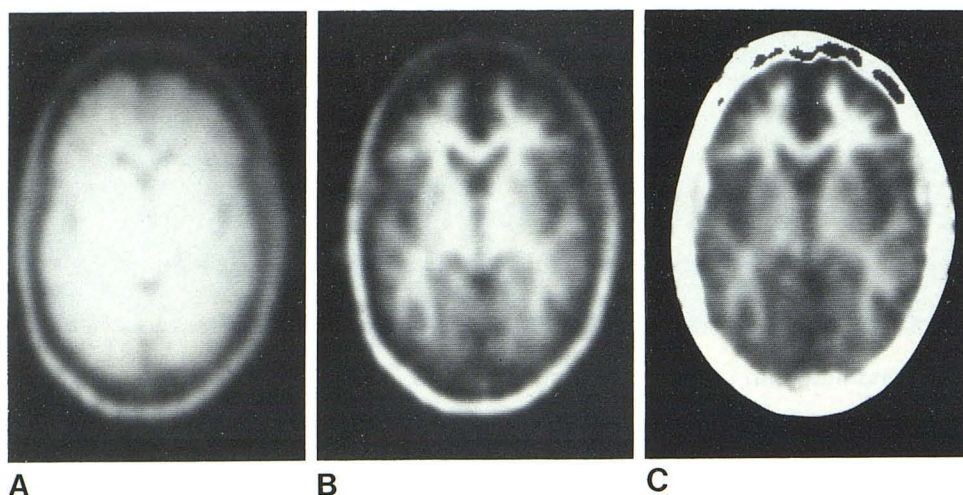
Fig. 1.—Approximate PD (A) and IR (B) images and computed T_1 rate map (C) at ventricular level in normal volunteer.
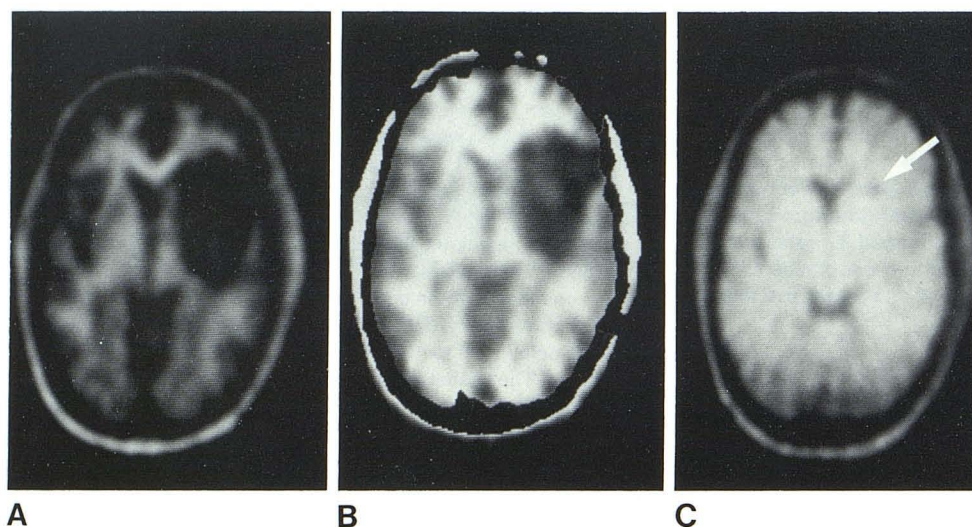

Fig. 2.—IR (A), T_1 rate map (B), and PD image (C) from patient with suspected right parietal glioma. Small area of diminished image intensity (*arrow*).
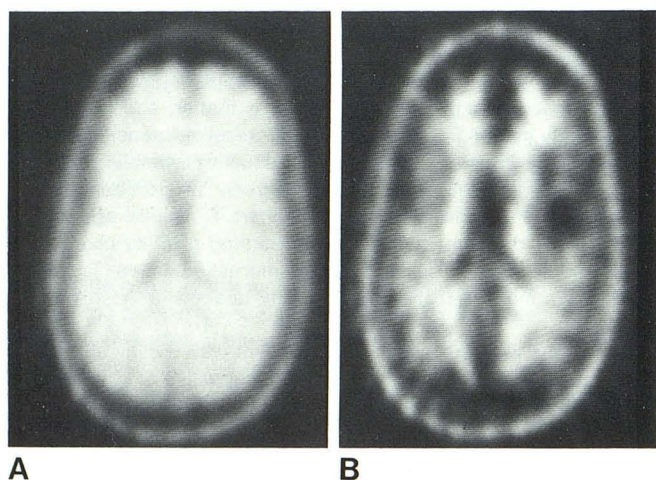

Fig. 3.—PD (A) and IR (B) images in patient with biopsy-proven grade II astrocytoma in right hemisphere.

ologic confirmation was not obtained. The IR image (fig. 2A) and T_1 map (fig. 2B) demonstrate the right parietal lesion as a region of decreased signal intensity consistent with prolonged T_1. The PD image (fig. 2C) does not demonstrate this pattern. The small area of decreased image intensity may represent either decreased mobile proton density or, more likely, a focal area of markedly prolonged T_1.

Figure 3 displays images from a patient with grade II astrocytoma. On the IR image (fig. 3B) the lesion appears as a central region of marked decreased signal intensity surrounded by a zone of lesser reduction in signal. While some of the reduced signal may be ascribable to normal sylvian cortex, this pattern may represent one of primary tumor with surrounding edema. The PD image (fig. 3A) fails to demonstrate this pattern.

Figure 4 presents data from a patient with a surgically confirmed olfactory groove meningioma. The CT image (fig. 4C) demonstrates an enhancing midline lesion with associated bifrontal and temporal cerebral edema. The IR image (fig. 4B) depicts the edema as a region of markedly decreased signal intensity corresponding to a

Fig. 4.—PD (A), IR (B), and CT (C) images at corresponding levels in patient with midline subfrontal meningioma.

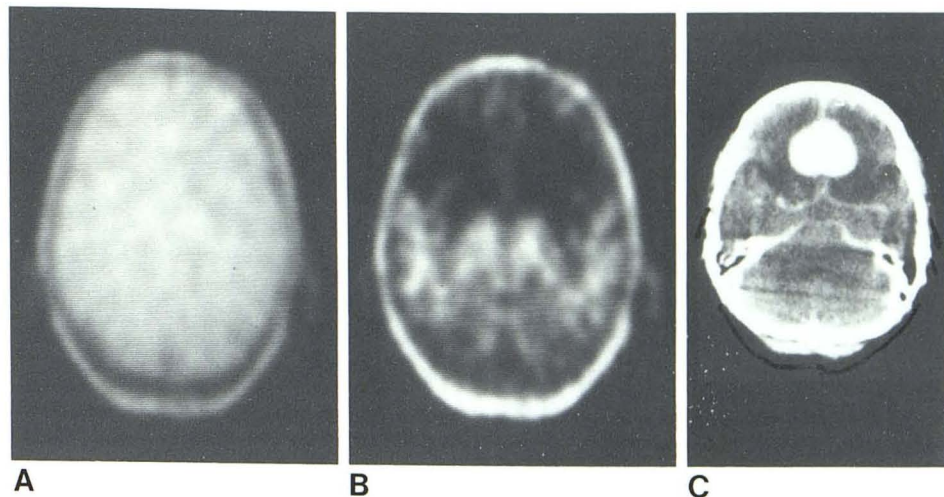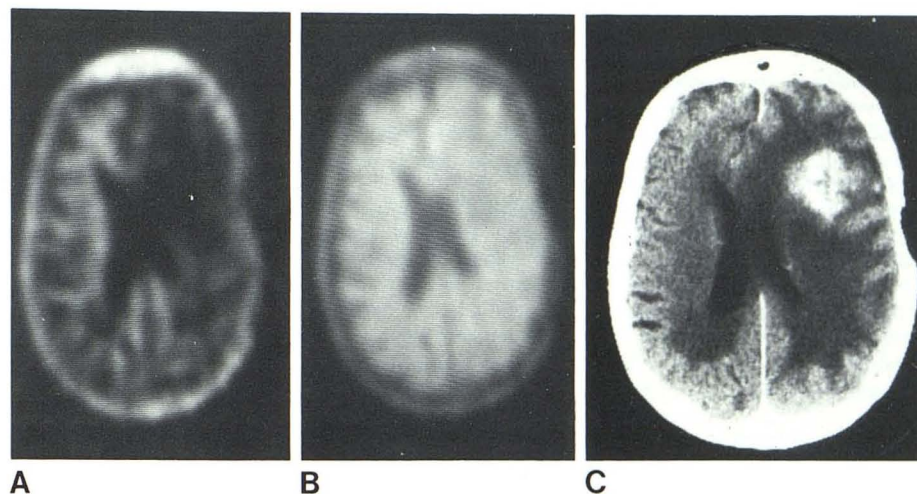A   B   C

Fig. 5.—Images from patient with histologically proven radiation necrosis. CT image (C) demonstrates enhancing lesion and marked left-sided edema. IR image (A) has heterogeneous decrease in signal intensity while PD image (B) is essentially normal except for mass effect.

A   B   C

prolonged T_1. The midline lesion has somewhat greater signal intensity, corresponding to shorter T_1 values, which nevertheless are longer than T_1 values of normal brain. The signal intensity on the PD image (fig. 4A) is slightly reduced within subcortical white matter, but differentiation between tumor and edema is not apparent.

Images in figure 5 were obtained from a patient with metastatic breast carcinoma to the left parietal calvaria and scalp. Several years after surgical resection and radiation therapy of about 6,500 rad (65 Gy) to the surgical site, the patient developed right-sided weakness and aphasia. The CT image (fig. 5C) shows an enhancing lesion in the left posterior frontal lobe surrounded by holohemispheric marked edema; localized edema is also evident in the right periventricular white matter. The IR image (fig. 5A) at the same level demonstrates a large area of heterogeneous decrease in signal intensity. The PD image (fig. 5B) has no significant side-to-side difference in signal intensity. All studies demonstrate the mass effect and postoperative changes.

In a patient stable and asymptomatic 2 years after surgical resection of a left frontal astrocytoma, the IR image (fig. 6A) shows a region of decreased signal intensity consistent with a prolonged

T_1 in the left frontal lobe; however, the lesion is not seen on the PD (fig. 6B) image. The CT image (fig. 6C) at the same level has a corresponding region of decreased x-ray attenuation. The abnormality, compatible with a surgical defect at the excisional biopsy site, is more clearly demonstrated on the IR image.

In all seven patient studies, IR images demonstrated lesions as regions of decreased signal intensity. The T_1 values of these lesions were significantly prolonged compared with values for contralateral normal tissue. The percentage increase in T_1 was 141%–191% of normal values. The absolute values for T_1, however, overlapped between the various tumors as well as with other pathologic processes.

From these preliminary data we conclude that IR NMR imaging is a sensitive method, albeit of low specificity, for the detection of tumors and other related CNS pathology; this is consonant with the experience of other investigators [6]. Using T_1 data, the specificity for lesion detection is low, since values for tumors overlap with values obtained from other lesions. With our present techniques, proton density imaging fails to provide additional diagnostic information. It is anticipated that the addition of T_2 imaging will provide the specificity required for in vivo tumor characterization.
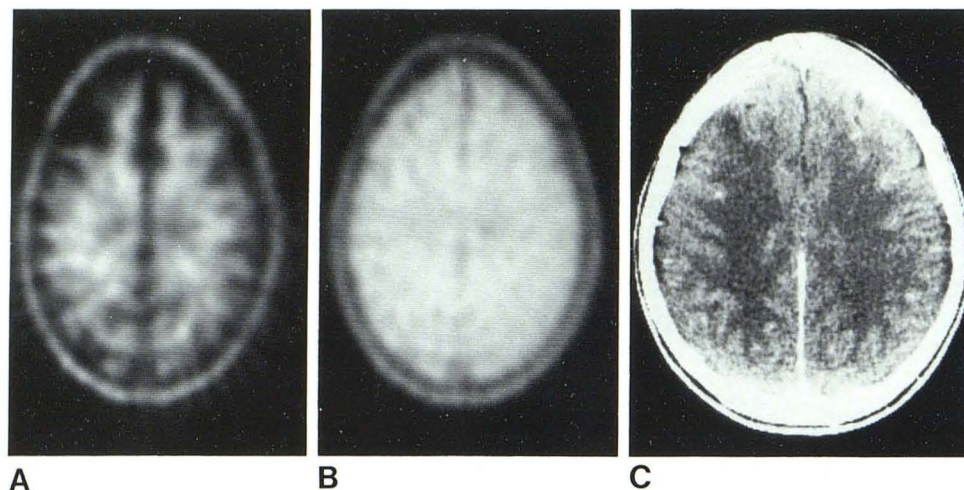
A   B   C

Fig. 6.—IR (**A**), PD (**B**), and CT (**C**) images from patient with resected left frontal astrocytoma. At corresponding level, IR image demonstrates extent of abnormality more clearly than CT.

REFERENCES

1. Damadian R. Tumor detection by nuclear magnetic resonance. *Science* **1971**;171:1151–1153
2. Hollis DP, Saryan LA, Morris HP. A nuclear magnetic resonance study of water in two Morris hepatomas. *Johns Hopkins Med J* **1972**;131:441–444
3. Hollis DP, Economou JS, Parks LC, Eggleston JC, Saryan LA, Czeisler JL. Nuclear magnetic resonance studies of several experimental and human malignant tumors. *Cancer Res*

1973;33:2156–2160
4. Saryan A, Hollis DP, Economou JS. Nuclear magnetic resonance studies of cancer. IV. Correlation of water content with tissue relaxation times. *JNCI* **1974**;52:599–602
5. Pykett IL, Rosen BR, Buonanno FS, Brady TJ. Measurement of spin-lattice relaxation times in nuclear magnetic resonance imaging. *Phys Med Biol* (in press)
6. Bydder GM, Steiner RE, Young IR, et al. Clinical NMR imaging of the brain: 140 cases. *AJNR* **1982**;3:459–480, *AJR* **1982**;139:215–236